

Geometric magnetoconductance dips by edge roughness in graphene nanoribbons

HENGYI XU¹, T. HEINZEL¹ and I. V. ZOZOULENKO²

¹ *Condensed Matter Physics Laboratory, Heinrich-Heine-Universität, Universitätsstr.1, 40225 Düsseldorf, Germany*

² *Solid State Electronics, Department of Science and Technology, Linköping University, 60174 Norrköping, Sweden*

PACS 81.05.ue – Graphene

PACS 73.23.-b – Electronic transport in mesoscopic systems

PACS 72.10.Fk – Scattering by point defects, dislocations, surfaces, and other imperfections

Abstract –The magnetoconductance of graphene nanoribbons with rough zigzag and armchair edges is studied by numerical simulations. nanoribbons with sufficiently small bulk disorder show a pronounced magnetoconductance minimum at cyclotron radii close to the ribbon width, in close analogy to the *wire peak* observed in conventional semiconductor quantum wires. In zigzag nanoribbons, this feature becomes visible only above a threshold amplitude of the edge roughness, as a consequence of the reduced current density close to the edges.

Graphene, i.e. a single layer of graphite, possesses an energy dispersion close to the charge neutrality point which is equivalent to the Dirac dispersion for massless fermions. [1, 2] This property has raised tremendous activities in fundamental research in the past few years, while the high room temperature electron mobility [3] of up to $20,000 \text{ cm}^2/\text{Vs}$ together with excellent mechanical properties has raised hopes for novel electronics applications. One key element of graphene nanostructures and devices are ribbons with submicron width W , also known as *graphene nanoribbons* (GNRs). It is well established that in GNRs, edge disorder can contribute significantly to the scattering [4–7] which is governed in wide structures by a combination of scattering at charged impurities and resonant scattering at short-range defects. [8, 9] Furthermore, edge roughness has been suggested as the source of the transport gap in narrow GNRs around the charge neutrality point. [7, 10–12] It would therefore be desirable to be able to characterize and quantify the edge roughness in GNRs via transport experiments. Conventional quantum wires made from, e.g., III/V semiconductors, show a characteristic magnetoresistance maximum at a perpendicular magnetic field which corresponds to a cyclotron radius $r_c \approx 0.55W$, commonly referred to as *wire peak*, [13] which can be interpreted as an enhanced diffusive scattering when the classical electron trajectory grazes at the wire edge. [13, 14] Within a quantum picture, the reduced conductance emerges from a homogenized contribution of the occupied wire modes to the overall conductivity. [14] Since

the strength of this effect depends on the parameters that characterize the edge roughness, namely its amplitude and correlation length which in turn determine the specularity of the edge scattering, [13, 14] the wire peak is routinely used to characterize the edge roughness. [13, 15–17] We are not aware of any observation of a similar structure in GNRs, where magnetoresistance peaks in the parameter range of interest are absent. [18–21] This difference between GNRs and conventional quantum wires has remained unexplained. The goal of the present paper is to fill this gap and discuss theoretically the edge roughness induced magnetoconductance dip (ERID) in GNRs. Our results show that this structure should be observable in GNRs as well provided the bulk disorder is sufficiently low. Furthermore, in zigzag GNRs, the structure is strongly suppressed at small edge disorder amplitudes.

We start with perfect armchair or zigzag nanoribbons oriented in x-direction and of width W in y-direction. Edge roughness is simulated at both edges by missing atoms. It is parameterized by the maximum number δ of missing atoms in y-direction from the edges into the GNR, and by the correlation length ξ . The positions of the notches in x-direction are chosen randomly with a probability p , while their individual central depth d^c is distributed equally between 0 and δ . Then the atoms around the defect centers are removed following the Gaussian-type shape such that the superimposed notches produce the

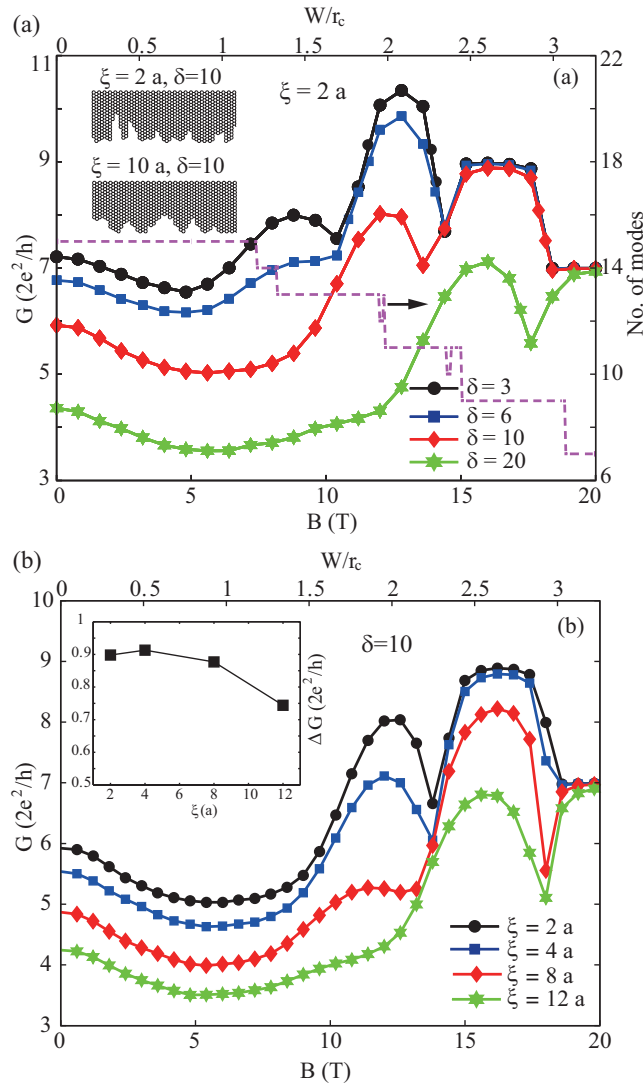


Fig. 1: (Colour online) Magnetoconductance of armchair GNRs (width 50 nm, length 220 nm) as a function of the edge roughness parameters δ (a) and ξ (b). Each trace is averaged over 500 edge configurations. The dashed lines show the number of occupied subbands. Inset in (a): typical edge profiles for specific parameter values. Inset in (b): amplitude of the ERID as a function of ξ .

number of missing atoms at edge site x_j

$$d(x_j) = \sum_{i=1}^{N_c} d_i^c \exp\left(-\frac{|x_i - x_j|^2}{2\xi^2}\right) \quad (1)$$

Here, $N_c = p \cdot N_{atom}$ is the number of notch centers with N_{atom} being the number of carbon atoms along the edges. The roughness patterns on both edges are uncorrelated. Typical structures are shown for one edge in the inset of fig. 1 (a).

Besides the edge roughness, we also study the ERID effect under the influence of bulk disorder which is modeled

by the widely used random Gaussian potential [25, 30]

$$V_i = \sum_{i'=1}^{N_{imp}} U_{i'} \exp\left(-\frac{|\mathbf{r}_i - \mathbf{r}_{i'}|^2}{2\Lambda^2}\right) \quad (2)$$

The potential heights U_i are uniformly distributed in the range $U_i \in [-\Delta, \Delta]$ where Δ denotes the maximum potential height. The potential decay depends on the site-site distance $|\mathbf{r}_i - \mathbf{r}_j|$ and the correlation length Λ . We refer to the case $\Lambda = a$ (appropriate for the absorbed neutral impurities) as short-range scattering, and to the case $\Lambda \gg a$ (appropriate for the remote charged impurities) as long-range scattering, with $a = 0.142$ nm being the C-C bond length.

Our calculations are based on the tight-binding Hamiltonian of GNRs

$$H = \sum_{i \neq j} t_{ij} c_i^\dagger c_j + \sum_i V_i c_i^\dagger c_i \quad (3)$$

with the hopping energy $t_{ij} = t = -2.7$ eV between the nearest neighboring carbon atoms at zero magnetic field. The perpendicular magnetic field is incorporated via Peierls' substitution $t_{ij} \rightarrow t_{ij} e^{ie/\hbar \int_i^j \mathbf{A} \cdot d\mathbf{l}}$ with the vector potential $\mathbf{A} = (-By, 0, 0)$ in the Landau gauge.

The conductance of GNRs is calculated with Landauer-Büttiker formula $G = 2e^2/hT(E_F)$, where the transmission $T(E_F)$ is computed with the aid of the recursive Green's function technique [6]. Throughout this work, the Fermi energy $E_F = 0.1t$ corresponding to an electron density of $n = 5.3 \times 10^{16} \text{ m}^{-2}$ is used. The Fermi wavelength λ_F is obtained from the linear band relation $E_F = \hbar v_F k_F$ and $\lambda_F = 2\pi/k_F$ with the Fermi velocity $v_F = 3ta/2\hbar$. The cyclotron radius is given by $r_c = \hbar k_F/eB$.

Fig. 1 shows the results for the magnetoconductance $G(B)$ of armchair GNRs of width $W = 50$ nm and length $L = 220$ nm for various values of the edge roughness parameters and in the absence of bulk disorder. As the magnetic field is increased from zero, $G(B)$ decreases and forms a broad minimum, the ERID, at $B_{min} \approx 5$ T corresponding to $W/r_c \approx 0.8$. By varying W in the simulations, we find that B_{min} is nearly inversely proportional to the GNR width W (not shown). This structure is the analogue of the so-called *wire peak* observed in conventional semiconductor quantum wires. [13] The amplitude of the ERID depends only weakly on the edge roughness amplitude δ , Fig. 1(a), and decreases as the correlation length of the roughness ξ is increased, Fig. 1(b). Outside the dip, a substantial increase of the conductance follows as B is increased, corresponding to the positive magnetoconductance observed in recent experiments. [18, 20] As the magnetic field is increased further beyond ≈ 12 T, oscillatory structures appear which reflect the magnetodepletion of the GNR modes and are of no further interest here. We note that the effective widths of GNRs are reduced by rough edges such that their signature in the magnetoconductance is slightly displaced with respect to the magnetodepletion of modes in defect-free GNRs. The ERID

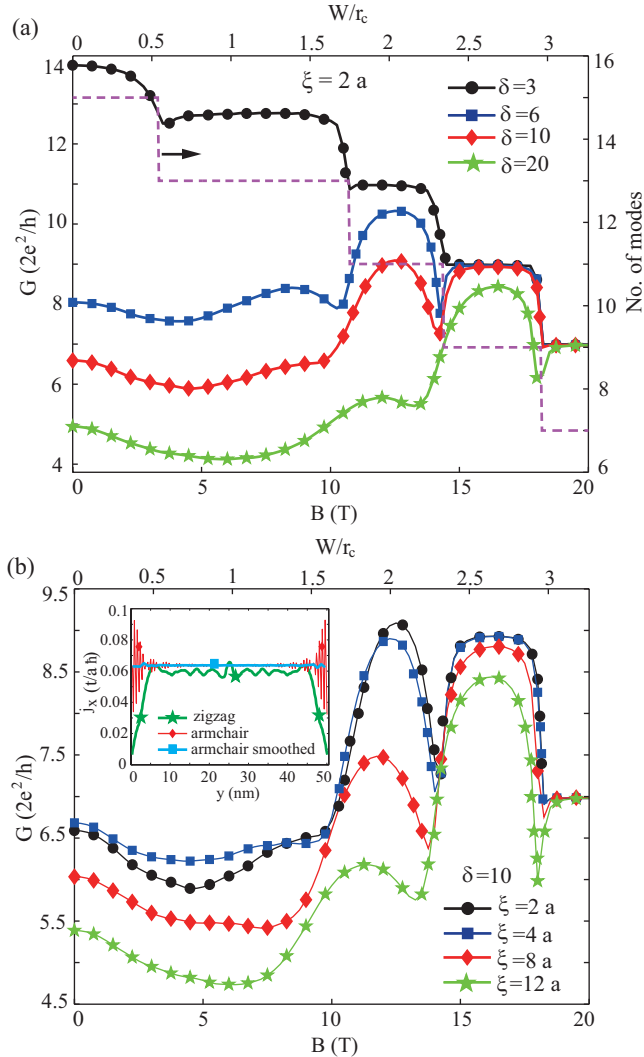


Fig. 2: (Colour online) Magnetoconductance of a GNR with zigzag edges and otherwise identical parameters to those in Fig. 1, for various edge disorder amplitudes and a fixed correlation length of $\xi = 2a$ (a), where the dashed line denotes the number of occupied modes, and for different correlation lengths at a disorder amplitude of $\delta = 10$ (b). The inset in (b) shows the cross-sectional current density for zigzag and armchair GNRs with perfect edges.

occurs in an interval where the number of occupied modes does not change much, which indicates that the structure is not related to the diamagnetic shift of the modes. This behavior is in qualitative agreement with the results of the quantum treatment of the wire peak in conventional quantum wires by Akera and Ando. [14]

Fig. 2 shows the corresponding results for zigzag GNRs. Again, the ERID structures are observed at cyclotron radii somewhat larger than W , but distinct differences to armchair GNRs can be identified. First of all, at $B = 0$, the conductance suppression by the edge disorder is less pronounced as compared to armchair GNRs. This represents the well-known reduced sensitivity to edge disorder

of zigzag GNRs compared to armchair GNRs. [4]. In addition, at small disorder amplitudes, e.g. for $\delta = 3$, uppermost trace in Fig. 2(a), the ERID is absent and the magnetoconductance reflects just the depopulation of the modes. As δ increases to 6, the ERID becomes visible, and its amplitude approaches that one observed in armchair GNRs as δ is increased. As ξ is increased at an amplitude of $\delta = 10$, Fig. 2 (b), the ERID amplitude develops nonmonotonically and shows a minimum around $\xi = 4a$. For larger correlation lengths, the ERID develops an asymmetric shape.

Apparently, compared to armchair GNRs, the magnetoconductance in zigzag GNRs is less sensitive to edge disorder for small disorder amplitudes. In order to interpret this difference, we take a look at the current density distribution $j_x(y)$ in GNRs with perfect edges, see the inset in Fig. 2 (b). The current density of armchair GNRs oscillates as a function of the site index (red trace), which is a consequence of the alternating character of the wave functions. Averaging over 4 adjacent atoms (blue trace) however shows that the current density is almost homogeneously distributed over the cross section. In zigzag GNRs, however, the current density is strongly suppressed in an interval extending about ≈ 5 nm from the edge into the bulk. This current density suppression, which has been reported earlier, [26] suggests that zigzag GNRs are less sensitive to edge disorder, in particular for disorder amplitudes below ≈ 5 nm for the Fermi energy considered here, which is in good qualitative agreement with the magnetoconductance simulations. Furthermore, it has been shown that in the single-mode regime in zero magnetic field, the conductance of the zigzag GNRs remains practically unaffected by the edge disorder [4]. In this case, the propagating channels in the zigzag GNRs are edge states flowing on the opposite boundaries [28,29] such that the backscattering is suppressed. We believe that this mechanism is not relevant in our study since we are in the multimode regime where the special character of the edge state should be insignificant. It would thus be interesting to study the magnetoconductance very in close proximity to the charge neutrality point. Our numerical method is an impractical tool for such a study due to the onset of Coulomb blockade effects as the Fermi energy is reduced. [27] We did, however, vary the number of occupied subbands at fixed Fermi energy by changing W and found that the ERID remains located close to $r_c = W$.

To discuss implications regarding the experimental observability of the ERID, we first study the effect of bulk disorder. The edge disorder of an armchair GNR is fixed to the parameters $\delta = 10$ and $\xi = 2a$ as used in Fig. 1. Fig. 3 (a) shows the magnetoconductance for various values of the bulk disorder potential amplitudes Δ , for short-range disorder ($\Lambda = a$) and with the impurity density $n_{imp} = 8 \times 10^{12} \text{cm}^{-2}$. As Δ gets larger, the absolute amplitude of the ERID gets suppressed while its position remains constant. In addition, a small conductance dip emerges at $B = 0$ as the bulk disorder is increased. We in-

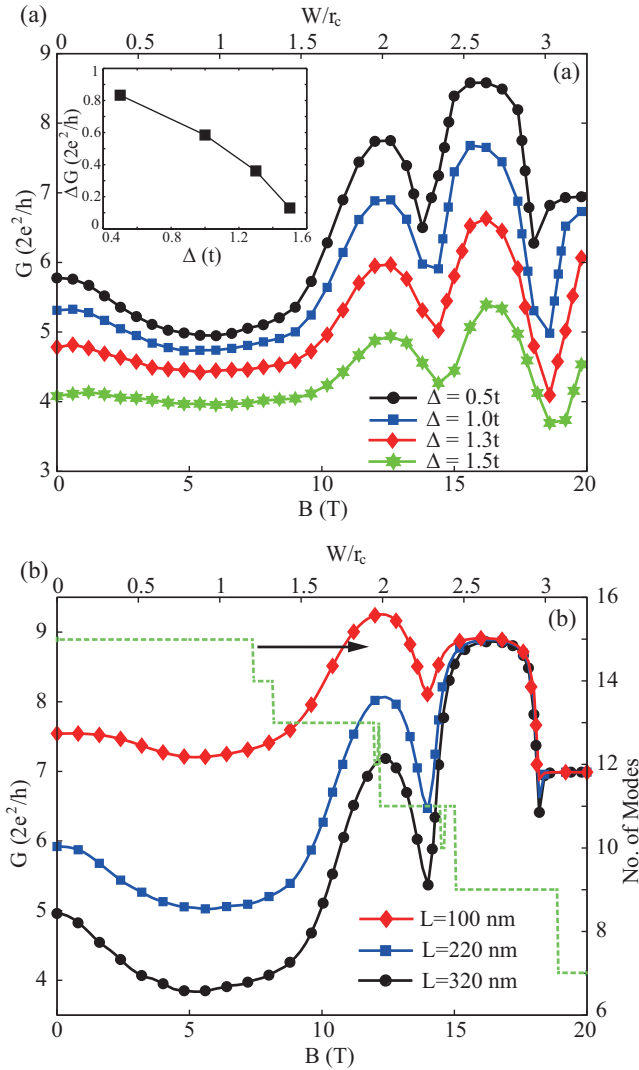


Fig. 3: (Colour on-line) (a) Effect of bulk disorder on the edge roughness induced magnetoconductance dip in armchair GNRs, averaged over 500 configurations. The width and length of GNR are 50 nm and 220 nm, respectively. The edge disorder parameters are $\delta = 10$ and $\xi = 2a$, while the bulk disorder is varied by tuning impurity center height Δ . The inset shows the ERID amplitude as a function of Δ . (b) Length dependence of the magnetoconductance.

terpret this as the onset of bulk-disorder induced weak localization. This behavior remains the same for long range potentials ($\Lambda = 32a$, not shown).

Second, the length dependence of the ERID is studied. As the length L of the GNR is increased from 100 nm to 200 nm, the ERID amplitude increases and tends to saturate as L is increased further. We take this as an indication that the system goes from the ballistic into the diffusive regime around a length of 200 nm. We note that in all cases studied here, the localization length ℓ_{loc} is larger than L . For the case shown in Fig. 3 (b), $\ell_{loc} = 2\mu\text{m}$ is found by fitting the scaling law $\ln(1+1/g) = L/\ell_{loc}$ with g denoting the dimensionless conductance $g = G/(e^2/\pi\hbar)$.

[31, 32] For GNRs with $L > \ell_{loc}$, the conductance would be exponentially suppressed.

These investigations allow us to draw some conclusions regarding the observability of the ERID in GNRs in experiments and concerning the suitability of this effect to characterize the edge roughness. It has emerged that the ERID can be observed in GNRs only if the bulk disorder level is sufficiently low. This may not be the case in present experimental implementations. Typical experimental edge roughness amplitudes are in the range of 1-10 missing atoms, which is the range where the wire peak should be observable in armchair GNRs provided the correlation length of the edge roughness remains small, i.e., of the order of the Fermi wavelength or below. In zigzag GNRs, on the other hand, the ERID will be only visible if the edge roughness amplitude is not small compared to the interval of suppressed current density at the GNR edges, i.e. $\delta \geq 6$ for the parameter range studied here. Like in conventional quantum wires, scattering at the edges gets less diffusive if the roughness becomes smoother which suppresses the ERID. Furthermore, the GNR lengths should be smaller than the localization length but well within the diffusive regime for maximum visibility. We note that there is no dephasing mechanism in our model. In real samples with finite dephasing time, the conductance around $B=0$ will increase due to the suppression of weak localization.

In summary, we have studied the magnetotransport properties of both armchair and zigzag GNRs in the presence of edge disorder. In both types of GNRs, an edge roughness - induced conductance minimum is found at cyclotron radii corresponding roughly to the GNR width, provided the edge disorder has a correlation length not much larger than the Fermi wavelength and the bulk disorder is sufficiently low. The effect is most visible in the diffusive regime. This magnetoconductance structure is similar in character to that one observed at conventional, rough quantum wires. Furthermore, in zigzag GNRs, it gets suppressed as the edge disorder amplitude drops below the spatial extension of the reduced current density.

H.X. and T.H. acknowledge financial support from Heinrich-Heine-Universität Düsseldorf

REFERENCES

- [1] NOVOSELOV K. S., GEIM A. K., MOROZOV S. V., JIANG D., KATSNELSON M. I. and GRIGORIEVA I. V., *Nature*, **438** (2005) 197.
- [2] NETO A. H. C., GUINEA F., PERES N. M. R., NOVOSELOV K. S. and GEIM A. K., *Rev. Mod. Phys.*, **81** (2009) 109.
- [3] MOROZOV S. V., NOVOSELOV K. S., KATSNELSON M. I., SCHEIN F., ELIAS D. C., JASZCZAK J. A. and GEIM A. K., *Phys. Rev. Lett.*, **100** (2008) 016602.
- [4] ARESHKIN D. A., GUNLYCKE D. and WHITE C. T., *Nano Lett.*, **7** (2007) 204.

- [5] EVALDSSON M., IHNATSENKA S. and ZOZOULENKO I. V., *Phys. Rev. B*, **77** (2008) 165306. **57** (1985) 287.
- [6] XU H., HEINZEL T., EVALDSSON M. and ZOZOULENKO I. V., *Phys. Rev. B*, **77** (2008) 245401.
- [7] HAN M. Y., OZYILMAZ B., ZHANG Y. and KIM P., *Phys. Rev. Lett.*, **98** (2007) 206805.
- [8] PERES N. M. R., *Rev. Mod. Phys.*, **82** (2011) 2673.
- [9] SARMA S. D., ADAM S., HWANG E. H. and ROSSO E., *Rev. Mod. Phys.*, **83** (2011) 407.
- [10] STAMPFER C., GUETTINGER J., HELLMUELLER S., MOLITOR F., ENSSLIN K. and IHN T., *Phys. Rev. Lett.*, **102** (2009) 056403.
- [11] LIU X. L., OOSTINGA J. B., MORPURGO A. F. and VANDERSYPEN L. M. K., *Phys. Rev. B*, **80** (2009) 121407.
- [12] TODD K., CHOU H. T., AMASHA S. and GOLDBABER-GORDON D., *Nano Lett.*, **9** (2009) 416.
- [13] THORNTON T. J., ROUKES M. L., SCHERER A. and VAN DE GAAG B. P., *Phys. Rev. Lett.*, **63** (1989) 2128.
- [14] AKERA H. and ANDO T., *Phys. Rev. B*, **43** (1991) 11676.
- [15] LETTAU C., WENDEL M., SCHMELLER A., HANSEN W., KOTTHAUS J. P., KLEIN W., TRAEINKLE G., WEIMANN G. and HOLLAND M., *Phys. Rev. B*, **50** (1994) 2432.
- [16] SCHÄPERS T., GUZENKO V. A., PALA M. G., ZÜLICHE U., GOVERNALE M., KNOBBE J. and HARDTDEGEN H., *Phys. Rev. B*, **74** (2006) 081301.
- [17] GILBERTSON A. M., FEARN M., KORMÁNYOS A., READ D. E., LAMBERT C. J., EMENY M. T., ASHLEY T., SOLIN S. A. and COHEN L. F., *Phys. Rev. B*, **83** (2011) 075304.
- [18] POUMIROL J.-M., CRESTI A., ROCHE S., ESCOFFIER W., GOIRAN M., WANG X., LI X., DAI H. and RAQUET B., *Phys. Rev. B*, **82** (2010) 041413.
- [19] BAI J., CHENG R., XIU F., LIAO L., WENG M., SHAILOS A., WANG K. L., HUANG Y. and DUAN X., *Nature Nanotech.*, **9** (2010) 655.
- [20] OOSTINGA J. B., SACEPE B., CRACIUN M. F. and MORPURGO A. F., *Phys. Rev. B*, **81** (2010) 193408.
- [21] RIBEIRO R., POUMIROL J.-M., CRESTI A., ESCOFFIER W., GOIRAN M., BROTO J.-M., ROCHE S. and RAQUET B., *arXiv:1102.3300v1[cond-mat.mes.hall]*, (2011).
- [22] ADAM S., BROUWER P. W. and SARMA S. D., *Phys. Rev. B*, **79** (2009) 201404.
- [23] KLOS J. W., SHYLAU A. A., ZOZOULENKO I. V., XU H. and HEINZEL T., *Phys. Rev. B*, **80** (2009) 245432.
- [24] RYCERZ A., TWORZYDLO J. and BEENAKKER C. W. J., *Europhys. Lett.*, **79** (2007) 57003.
- [25] LEWENKOPF C. H., MUCCILOLO E. R. and CASTRO NETO A. H., *Phys. Rev. B*, **77** (2008) 081410.
- [26] ZARBO L. P. and NIKOLIC B. K., *Europhys. Lett.*, **80** (2007) 47001.
- [27] DRÖSCHER S., KNOWLES H., MEIR Y., ENSSLIN K. and IHN T. and NIKOLIC B. K., *Phys. Rev. B*, **84** (2011) 073405.
- [28] WAKABAYASHI K., FUJITA M., AJIKI H. and SIGRIST M., *Phys. Rev. B*, **59** (1999) 8271.
- [29] WAKABAYASHI K., TAKANE Y. and SIGRIST M., *Phys. Rev. Lett.*, **99** (2007) 036601.
- [30] BARDARSON J. H., TWORZYDLO J., BROUWER P. W., and BEENAKKER C. W. J., *Phys. Rev. Lett.*, **99** (2007) 106801.
- [31] XU H., HEINZEL T. and ZOZOULENKO I. V., *Phys. Rev. B*, **80** (2009) 045308.
- [32] LEE P. A. and RAMAKRISHNAN T. V., *Rev. Mod. Phys.*,